Corrosion Science 80 (2014) 318–330

Contents lists available at ScienceDirect

Corrosion Science

journal homepage: www.elsevier.com/locate/corsci

Corrosion of conductive polypyrrole: Effects of possibly formed galvanic cells

Kai Qi [a], Yubing Qiu [a,*], Zhenyu Chen [a,b], Xingpeng Guo [a,b,*]

[a] School of Chemistry and Chemical Engineering, Huazhong University of Science and Technology, Wuhan 430074, PR China
[b] Hubei Key Laboratory of Materials Chemistry and Service Failure, Wuhan 430074, PR China

ARTICLE INFO

Article history:
Received 30 June 2013
Accepted 28 November 2013
Available online 4 December 2013

Keywords:
A. Polymer
B. XPS
C. Potential parameters
C. Oxygen reduction

ABSTRACT

Some galvanic couples were designed with PPy films to simulate possibly formed corrosion cells on PPy. Their effects on the corrosion of PPy were investigated using electrochemical methods and XPS analysis. The results indicate that the PPy redox state difference cell just occurs in the initial corrosion period and can not be sustained on PPy. The H^+ ion and electrolyte concentration difference cells can be sustained on PPy but do not influence the corrosion of PPy. The oxygen concentration difference cell can also be sustained on PPy and severely accelerates the corrosion of PPy. The mechanism involved is discussed.

© 2013 Elsevier Ltd. All rights reserved.

1. Introduction

Polypyrrole (PPy) has been studied and used widely owing to its advantageous physical and chemical properties [1–8]. With regard to its applications, the stability of PPy is a key issue because PPy may undergo irreversible degradation and loss of performance in service environment [9,10], which is also considered as the corrosion of PPy according to the European Federation of Corrosion Working Party on Corrosion of Polymer Materials [11]. However, the corrosion mechanism of PPy is still not clearly understood.

The corrosion of PPy will decrease its conductivity [12–14] and electroactivity [15,16]. The changes of PPy structure and chemical components after corrosion have been studied using Fourier transform infrared spectroscopy (FTIR), X-ray photoelectron spectroscopy (XPS), ultraviolet–visible absorption spectroscopy (UV–Vis), Raman spectroscopy, atomic force microscope (AFM) and scanning electron microscope (SEM) analysis [17–19]. According to these researches, it is generally believed that the corrosion of PPy is induced by nucleophilic attack from H_2O, OH^-, CH_3OH or NH_3, etc. This corrosion not only destroys the conjugated structure of the PPy chains, but also results in the loss of electrochemical activity [20–25]. However, all these researches just consider the chemical action between PPy and media.

PPy has a large surface conjugated molecular structure and conducts through the activation of conjugated π electrons [26]. After being doped, it can reach the conductive level of metals. Moreover, PPy has similar charge transfer ability and electrochemical catalytic activity as metals, so it can act as a good interface for electrochemical redox reactions [27–31]. In this case, corrosion cells can be formed on PPy surfaces in electrolyte media, just like their formation on metals. If so, apart from the chemical action between PPy and media it may also suffer electrochemical corrosion. However, few studies involve this area.

According to our previous work [32,33], high concentrations of supporting electrolyte and low temperatures retard the corrosion of PPy in alkaline solutions. Dissolved oxygen (DO) can be reduced on PPy film, and high concentrations of DO accelerate PPy corrosion. At positive potentials vs. open circuit potential (OCP) the corrosion of PPy is promoted, while the corrosion of PPy is inhibited at negative potentials (vs. OCP). These features are quite similar to those experienced by metals in electrolyte solutions, which suggest that electrochemical processes may play an important role in the corrosion of PPy. However, we still do not know how corrosion cells are formed and maintained on the PPy in a free corrosion state, and also do not know their effects on the corrosion of PPy. Further research is still needed to verify the electrochemical mechanism in the corrosion of PPy.

In order to find what kinds of corrosion cells can be formed and sustained on PPy films, some galvanic couples, which were constructed with PPy film electrodes to simulate possibly formed corrosion cells on PPy, were studied using electrochemical methods. The effects of these galvanic couples on the conductivity and chemical components of the PPy electrodes were also

* Corresponding authors. Address: School of Chemistry and Chemical Engineering, Huazhong University of Science and Technology, Wuhan 430074, PR China (X. Guo). Tel.: +86 27 87543432; fax: +86 27 87543632.
E-mail addresses: qiuyubin@mail.hust.edu.cn (Y. Qiu), guoxp@mail.hust.edu.cn (X. Guo).

0010-938X/$ - see front matter © 2013 Elsevier Ltd. All rights reserved.
http://dx.doi.org/10.1016/j.corsci.2013.11.040

investigated using four probe conductivity test method and XPS analysis. A scanning electrochemical probe method was used to measure the change of potential distribution on PPy films to further verify the formation of corrosion cells on PPy films. The results will be helpful to make clear the electrochemical mechanism in the corrosion of PPy.

2. Experimental

Pyrrole (Py, SAFC®, 98+ %) used for the synthesis of PPy was distilled and kept refrigerated in the dark before use. Other reagents and chemicals were analytical grade and used as received. Solutions were prepared with deionized water, and all experiments were carried out at 25 ± 0.5 °C controlled with a water bath unless otherwise indicated. The pH of electrolytes was adjusted with 1 M HCl or NaOH solutions. All electrochemical tests were performed using a CS350 electrochemical workstation.

2.1. Electro-polymerization of PPy

A conventional three-electrode system in a single compartment cell was used to synthesise PPy films. The counter and reference electrodes were a large Pt foil and a saturated calomel electrode (SCE), respectively. A super 13Cr stainless steel plate was used as the working electrode with the chemical composition (wt.%): C 0.01, Si 0.23, Mn 0.42, Cr 12.0, Ni 5.4, Mo 1.9, P 0.014, S 0.001, V 0.06, Ti 0.09 and Fe for the balance. It was sealed by epoxy resins with 3.6 cm^2 of working area, gradually ground using silicon carbide paper up to 5000 grit and rinsed using ethanol and distilled water. Electro-polymerization of PPy film was performed at 750 mV (vs. SCE) in 0.1 M pyrrole aqueous solutions containing 0.1 M sodium *p*-toluenesulfonate (NapTS) supporting electrolyte and which had been deaerated by bubbling pure N_2 gas for 20 min before synthesis. The polymerization charge density was 4.0 C cm^{-2}. After the electro-polymerization, a black, smooth and uniform PPy/pTS film with metallic lustre was obtained on the stainless steel plate.

2.2. Preparation of the PPy electrode with glass substrate (glass//PPy/pTS electrode)

In order to eliminate the influence of the metal substrate on the electrochemical behaviour of PPy, a glass substrate was used to prepare the glass//PPy/pTS electrode, as shown in Fig. 1. The PPy/pTS film formed on the stainless steel substrate was carefully removed and cut to small pieces with a blade. A small piece of the PPy/pTS film was fixed on an insulated glass slide with an inert double faced adhesive tape. Then, a copper wire was connected to one end of the PPy film with the silver conductive adhesive, where the total connection resistance was less than 0.5 Ω. At last, the electric connection area was sealed with the silastic adhesive to form a working area (0.5 cm^2).

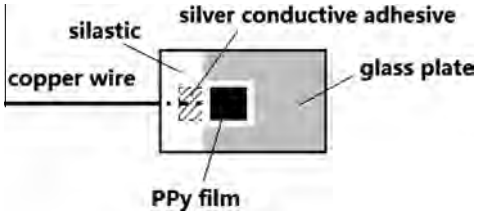

Fig. 1. Schematic of the glass//PPy electrode.

2.3. Tests in galvanic couples

Fig. 2 shows the schematic of the galvanic cells that was specially designed for this work. Table 1 lists the detailed conditions in the galvanic cells. The working and reference electrodes were two glass//PPy/pTS electrodes and a SCE, respectively. The galvanic current and potential were measured simultaneously with the CS350 electrochemical workstation which includes a zero-resistance ammeter (ZRA) for the galvanic current measurement. Under an open circuit state, the change of the open circuit potential (E_{OCP}) of each PPy electrode as a function of time was measured respectively in the corresponding galvanic cell.

2.4. Electrical conductivity (σ) measurement

The PPy films tested in the galvanic couples were cleaned in distilled water and then dried in a vacuum-desiccator for more than 12 h before the electrical conductivity measurement. The direct current (DC) conductivity in the PPy film was determined with a typical four probe method. A ST2253 digital four probe conductivity tester was employed for the electrical conductivity measurement with a linear 2 mm spacing arrangement of four tungsten carbide probes that contact with a tip diameter of 0.5 mm and elastic modified length. A special device allows the probes to settle vertically on the PPy film surface and press until a stable reading is obtained. The thickness of the PPy film was determined accurately using a digimatic outside micrometer with a resolution of 1 μm.

2.5. XPS analysis

XPS analysis was performed using a commercial VG Multilab 2000 system in order to find the changes of chemical structure and component in the PPy films tested in the galvanic couples. The base pressure in the experimental chamber was below 10^{-9} - mbar range. The spectra were measured using Al Kα (1486.6 eV) radiation, and the overall energy resolution was 0.45 eV. The surface charging effect during measurements was compensated by referencing the binding energy to the C 1s line of residual carbon at 284.6 eV. The N 1s level spectral decomposition was analyzed using background subtraction and a least-squares fitting programme.

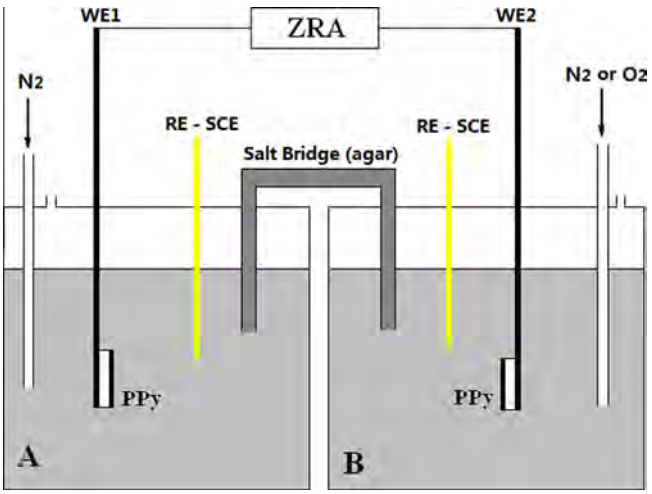

Fig. 2. Schematic of the designed galvanic cell.

www.spm.com.cn

Table 1
Detailed conditions in the galvanic cells.

		A cell	B cell
(1)	PPy	Polarised at −0.6 V (vs. SCE) for 10 min	Polarised at 0.6 V (vs. SCE) for 10 min
	[NaCl]	0.1 M	0.1 M
	pH	7	7
	DO	Deaerated with N_2	Deaerated with N_2
(2)	PPy	Freshly-made PPy film	Freshly-made PPy film
	[NaCl]	0.1 M	0.1 M
	pH	7	7
	DO	Deaerated with N_2	Aerated with O_2
(3)	PPy	Freshly-made PPy film	Freshly-made PPy film
	[NaCl]	0.1 M	0.1 M
	pH	9	2
	DO	Deaerated with N_2	Deaerated with N_2
(4)	PPy	Freshly-made PPy film	Freshly-made PPy film
	[NaCl]	1.0 M	0.1 M
	pH	7	7
	DO	Deaerated with N_2	Deaerated with N_2

2.6. Potential distribution measurement with a scanning electrochemical probe system

The potential distribution of a PPy film in aerated 0.1 M NaCl solutions was measured with a XMU-BY-1 scanning electrochemical workstation system (made by Xiamen University, China). The scanning microprobe system with an electrochemical cell is shown schematically in Fig. 3 [34]. The two micro-reference probes, i.e. B and C in Fig. 3, were made of platinum (Pt)/iridium (Ir) (10%) wires (Φ 0.10 mm), whose tips were etched in 2 M NaOH with an alternating current to provide a tip diameter of 5 μm. Movement of the micro-reference probe (C in Fig. 3) over the specimen surface was driven by two stepper motors controlled by a microcomputer, while measurements and data processing were performed by a self-compiled program, as described in Ref. [34].

The distance between the scanning micro-reference probe tip and the specimen surface was controlled accurately by a high-resolution piezoelectric stack/tube in the scanning tunneling microscope (STM) mode. Before the electrolyte was added into the electrochemical cell, the scanning probe was automatically brought to the PPy surface until the tunneling current was sensed, which indicates that the distance between the probe tip and the specimen surface is within a few nanometers. Then the scanning probe was accurately moved away 20 μm from the testing surface in order to minimize the possible scanning disturbance in the solution near the specimen surface.

All the measurements were carried out in a free corrosion state at room temperature (25 ± 2 °C). The potential distribution on the PPy surface in an area of 1 mm × 1 mm (256 × 256 points) was measured for about 20 min and presented as topographical 3D images.

3. Results

3.1. PPy redox state difference cell

As shown in Fig. 2, the PPy electrode in the cell A was polarised at −0.6 V vs. SCE for 10 min in deaerated 0.1 M NaCl to make it in a reduced state, while another PPy electrode in the cell B was polarised at 0.6 V vs. SCE for 10 min in deaerated 0.1 M NaCl to make it in an oxidized state. In this case, a PPy redox state difference cell was formed with the two PPy electrodes in different redox states.

Fig. 4 presents the changes of the galvanic current density (I_{couple}) and galvanic potential (E_{couple}) as a function of time (t) (I_{couple}-t and E_{couple}-t curves) in this PPy redox state difference cell. The changes of the E_{OCP} values of the two PPy electrodes as a

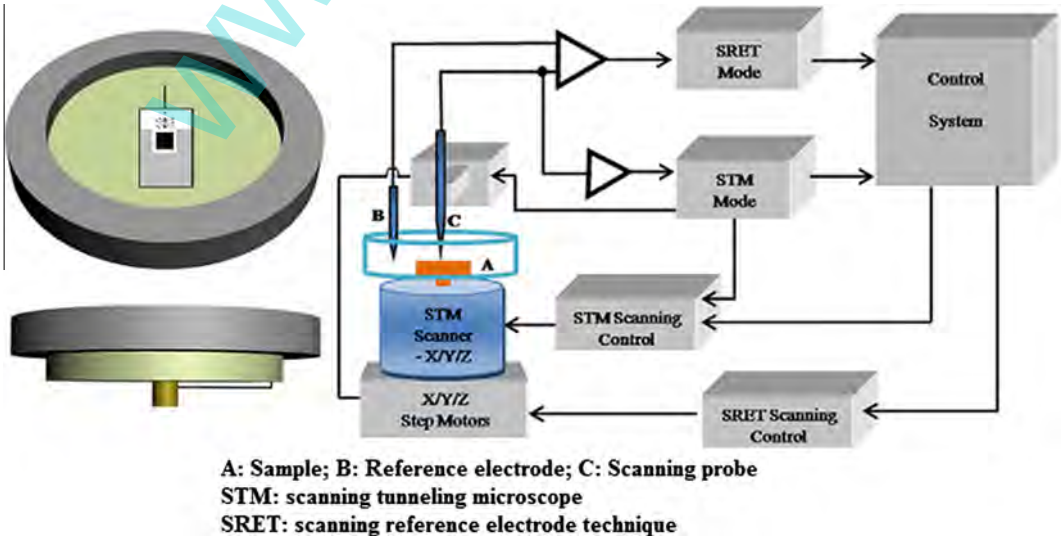

Fig. 3. Schematic of the scanning probe system with the electrochemical cell.

www.scm.com.cn

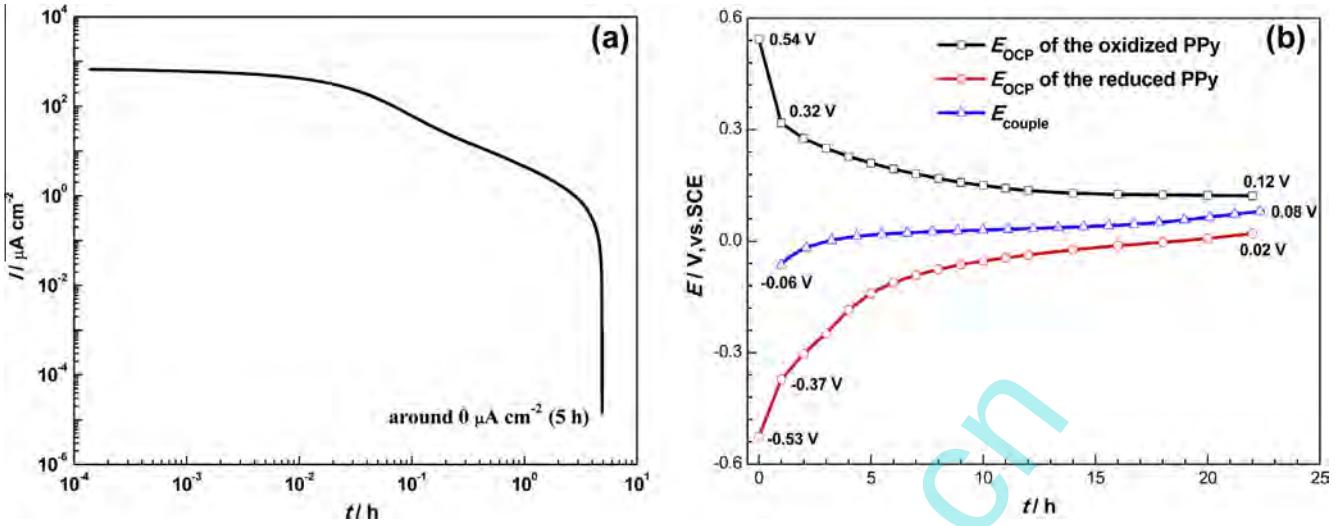

Fig. 4. (a) I_{couple}-t , (b) E_{couple}-t and E_{OCP}-t curves in the galvanic couple formed with PPy films in different redox states (deaerated 0.1 M NaCl, pH = 7, at 25 °C).

function of time (E_{OCP}-t curves) are also presented in Fig. 4(b) to shows their potential difference at the beginning of coupling and the approximate polarisation extent of each PPy electrode during the coupling period. As shown in Fig. 4(a), I_{couple} decreases quickly in the early period of coupling and then gradually reduces to around 0 μA cm^{-2} after about 5 h, suggesting that this kind of galvanic couple cannot be sustained for a long time. In Fig. 4(b), E_{couple} changes slightly during the whole coupling period, while the E_{OCP} values of the two PPy electrodes change slowly to approach each other. The potential difference between the two PPy electrodes is more than 1.0 V before they are coupled, which results in a large I_{couple} in the early period of coupling. With an increase in the coupling time (t_{couple}), the polarisation extent of each PPy electrode decreases largely, suggesting that the redox state difference between the two PPy electrodes is quickly eliminated with the polarisation effect. This makes I_{couple} decrease and gradually disappear.

3.2. Oxygen concentration difference cell

As shown in Fig. 2, two identical PPy film electrodes were placed respectively in the cell A and cell B (with 0.1 M NaCl, pH = 7). The two cells were firstly deaerated by bubbling N_2, while the I_{couple} resulting from the slight redox state difference between the two PPy electrodes decreased quickly to near 0 μA cm^{-2}. Then the cell B was aerated by continuously bubbling O_2, leaving the cell A deaerated by continuously bubbling N_2. In this case, an oxygen concentration difference cell was formed.

Fig. 5 presents the I_{couple}-t and E_{couple}-t curves of the oxygen concentration difference cell. The E_{OCP}-t curve of each PPy electrode in the cell A and B is also presented respectively in Fig. 5(b). As shown in Fig. 5(a), I_{couple} increases immediately as soon as O_2 is bubbled in the cell B and then gradually decreases to a relatively stable value (about 1.0 μA cm^{-2} for 19 h). The direction of I_{couple} and the E_{OCP} values in Fig. 5(b) indicate that the PPy electrode in the aerated solution acts as a cathode, while that in the deaerated solution acts as an anode. About 20 h later, as N_2 is bubbled again in the cell B, I_{couple} decreases to near 0 μA cm^{-2} within 1 h, suggesting that the oxygen concentration difference plays a key role in the formation of this galvanic couple. The I_{couple}-t curve of a test for 100 h, as shown in the inset of Fig. 5(a), further proves that the oxygen concentration difference cell can be sustained on PPy films.

In Fig. 5(b), the E_{OCP} of the PPy electrode in the aerated solution increases in the beginning period with O_2 bubbling, resulting in the rapid increase in I_{couple}, and then, gradually reaches a relatively stable value. However, the E_{OCP} of the PPy electrode in the deaerated solution decreases largely with time, which may result in the decrease in E_{couple}. This result will be discussed later.

Fig. 6 shows the changes in electrical conductivity (σ) with time for the PPy anode and cathode in the oxygen concentration difference cell ($\sigma_{o\text{-anode}}$ and $\sigma_{o\text{-cathode}}$) and those just immersed in the corresponding deaerated and aerated 0.1 M NaCl under free corrosion conditions ($\sigma_{deareated}$ and $\sigma_{areated}$). The electrical conductivity of the newly prepared PPy film (σ_0) is also given in Fig. 6 for comparison. It is seen that $\sigma_{o\text{-anode}}$ increases when t_{couple} = 20 h compared with σ_0, resulting from the oxidation of the PPy film under anodic polarisation. When t_{couple} increases to 40 h and 75 h, $\sigma_{o\text{-anode}}$ decreases obviously. This should be attributed to the break of PPy conjugated structure after a longtime anodic polarisation [33]. In addition, $\sigma_{deareated}$ decreases more slowly with time (t > 20 h) compared with $\sigma_{o\text{-anode}}$. Obviously, the longtime anodic polarisation (t > 20 h) with a small anodic current density still accelerates the corrosion of PPy. In the oxygen concentration difference cell, $\sigma_{o\text{-cathode}}$ decreases largely with t_{couple}, resulting from the reduction of the PPy film under cathodic polarisation. Apparently, the large decrease in $\sigma_{o\text{-cathode}}$ will increase the total resistance in the oxygen concentration difference cell and lead to the decrease of I_{couple}. Similarly, $\sigma_{areated}$ decreases much more slowly with time compared with $\sigma_{o\text{-cathode}}$, indicating that cathodic polarisation accelerates the loss of the conductivity of PPy. It should be noted that $\sigma_{deareated}$ decreases more slowly with the immersed time than $\sigma_{areated}$, suggesting that DO plays an important role in the corrosion of PPy [32].

Fig. 7 presents the high resolution XPS spectra of N 1s for the PPy anode and cathode in the oxygen concentration difference cell for 75 h and those just immersed in the corresponding solutions for the same time under free corrosion conditions. The XPS N 1s spectra can be deconvoluted into three components [32,35–38]: a $N^{\delta+}$ that is due to polarons or bipolarons, a —NH— that is the characteristic of pyrrolylium nitrogen, and a =N— resulting from deprotonation during corrosion. Thus, the ratio of each component's content to the total N content (N_{Total}) can be calculated from the XPS N 1s spectra. Table 2 gives the values of $N^{\delta+}/N_{Total}$ and =N—/N_{Total} for different PPy films obtained from Fig. 7. It is seen that in deaerated 0.1 M NaCl the =N—/N_{Total} ratio of the PPy anode (0.055) is larger than that of the PPy film just corroded under the free corrosion

www.scm.com.cn

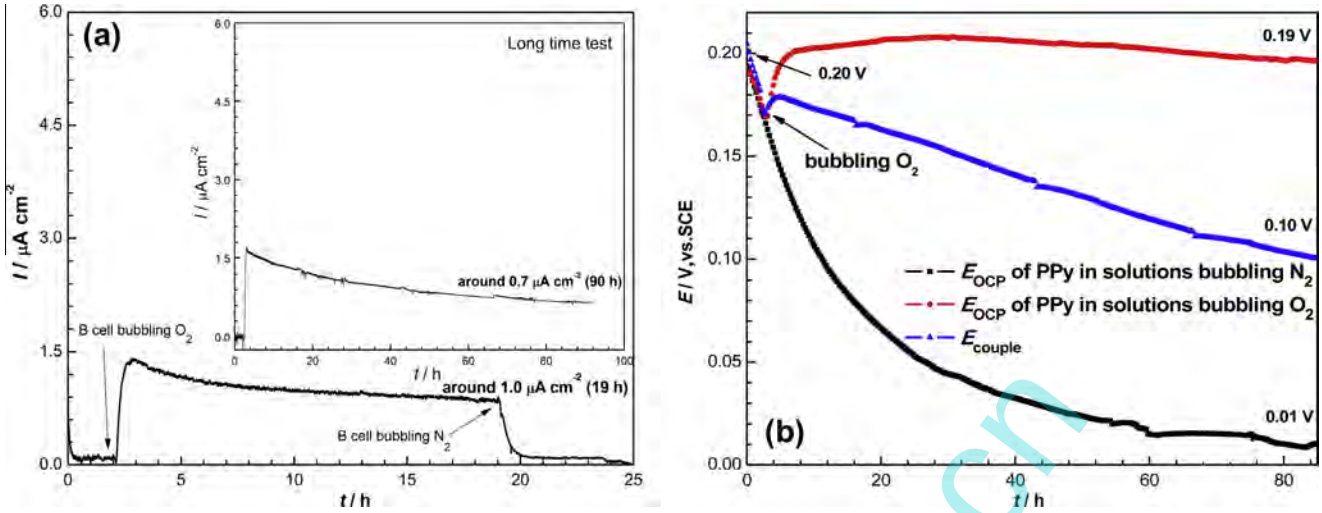

Fig. 5. (a) I_{couple}-t, (b) E_{couple}-t and E_{OCP}-t curves in the oxygen concentration difference cell (aerated and deaerated 0.1 M NaCl, pH = 7, at 25 °C. Inset is the I_{couple}-t curve of a test for 100 h).

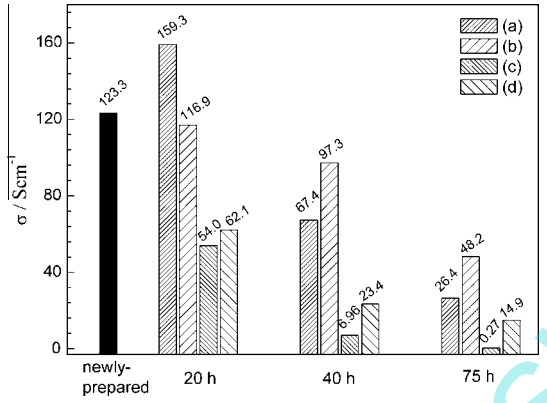

Fig. 6. Changes in electrical conductivity (σ) with time for (a) a PPy anode in the oxygen concentration difference cell in deaerated 0.1 M NaCl ($\sigma_{o\text{-anode}}$), (b) a PPy film immersed in deaerated 0.1 M NaCl ($\sigma_{deareated}$), (c) a PPy cathode in the oxygen concentration difference cell in aerated 0.1 M NaCl ($\sigma_{o\text{-cathode}}$) and (d) a PPy film immersed in aerated 0.1 M NaCl ($\sigma_{areated}$).

condition (0.034). This result indicates that the anodic polarisation accelerates the corrosion of the PPy anode and makes more PPy chains lose their conjugated structure. In this case, even though the anodic polarisation makes the $N^{\delta+}/N_{Total}$ ratio for the PPy anode increase ($N^{\delta+}/N_{Total}$ ratio rises from 0.173 to 0.283), the conductivity of the PPy anode still decreases obviously as shown in Fig. 6.

In aerated 0.1 M NaCl, the $=N-/N_{Total}$ ratio of the PPy film just corroded under the free corrosion condition (0.150) increases obviously compared with that in deaerated 0.1 M NaCl (0.034), which indicates that the free corrosion of PPy in aerated 0.1 M NaCl is much severer than that in deaerated 0.1 M NaCl. In the oxygen concentration difference cell, the $=N-/N_{Total}$ ratio of the PPy cathode decreases to 0.115, suggesting that the cathodic polarisation depresses the corrosion of the PPy cathode to some extent [33]. Meanwhile, the $N^{\delta+}/N_{Total}$ ratio of the PPy cathode (0.114) becomes smaller than that of the PPy film just corroded under the free corrosion condition (0.143). This is due to the reduction of the PPy cathode under cathodic polarisation. Apparently, the severe free corrosion and the reduction effect under cathodic polarisation make the PPy cathode lose its conductivity seriously, as shown in Fig. 6.

3.3. H^+ ion concentration difference cell

As shown in Fig. 2, two identical PPy film electrodes were placed respectively in the cell A (with deaerated 0.1 M NaCl, pH = 9) and the cell B (with deaerated 0.1 M NaCl, pH = 2) to form the H^+ ion concentration difference cell.

Fig. 8 gives the I_{couple}-t and E_{couple}-t curves of the H^+ ion concentration difference cell. The E_{OCP}-t curve of each PPy electrode in the cell A and B is also presented respectively in Fig. 8(b). As shown in Fig. 8(a), after a quick decrease in the early period of coupling, I_{couple} gradually reaches a relatively stable value within 1 h and still maintains around 0.4 μA cm^{-2} when t_{couple} = 20 h, indicating that the H^+ ion concentration difference cell can be sustained on PPy films. The direction of I_{couple} and the E_{OCP} values in Fig. 8(b) indicates that the PPy film electrode in the cell B (pH = 2) acts as a cathode and that in the cell A (pH = 9) acts as an anode.

In Fig. 8(b), the E_{OCP} of the PPy film electrode in the cell B (pH = 2) is more positive than that in the cell A (pH = 9). Both of the E_{OCP} firstly decreases with time and gradually reaches relatively stable in the same way, which may lead to the change in the E_{couple} with time.

Fig. 9 shows the electrical conductivity values for the PPy anode and cathode in the H^+ ion concentration difference cell for 40 h ($\sigma_{pH\text{-anode}}$ and $\sigma_{pH\text{-cathode}}$) and those just immersed in the corresponding solutions for the same time under free corrosion conditions ($\sigma_{pH=2}$ and $\sigma_{pH=9}$). It is seen that $\sigma_{pH\text{-anode}}$ and $\sigma_{pH=9}$ all decrease largely compared with σ_0 (see Fig. 6), which is due to the severe corrosion of PPy in alkaline solutions (pH = 9) [32]. In addition, $\sigma_{pH\text{-anode}}$ is larger than $\sigma_{pH=9}$, owing to the oxidation effect from the slight anodic polarisation, which is consistent with the result at 20 h in Fig. 6. However, $\sigma_{pH=2}$ becomes larger than σ_0, and $\sigma_{pH\text{-cathode}}$ decreases slightly compared with $\sigma_{pH=2}$. The increase in $\sigma_{pH=2}$ is due to the doping of H^+ ions to PPy in acid solutions (pH = 2) [39], while the slight decrease in $\sigma_{pH\text{-cathode}}$ should result from the reduction effect of the slight cathodic polarisation.

Fig. 10 presents the high resolution XPS spectra of N 1s for the PPy anode and cathode in the H^+ ion concentration difference cell for 40 h and those just immersed in the corresponding solutions for the same time under free corrosion conditions, where Table 3 gives the values of $N^{\delta+}/N_{Total}$ and $=N-/N_{Total}$ for the different PPy films obtained from Fig. 10. It is seen that in the alkaline deaerated 0.1 M NaCl (pH = 9) the two $=N-/N_{Total}$ ratios are close to each other ($=N-/N_{Total}$ ratio = 0.065 and 0.067, respectively) and much

www.spm.com.cn

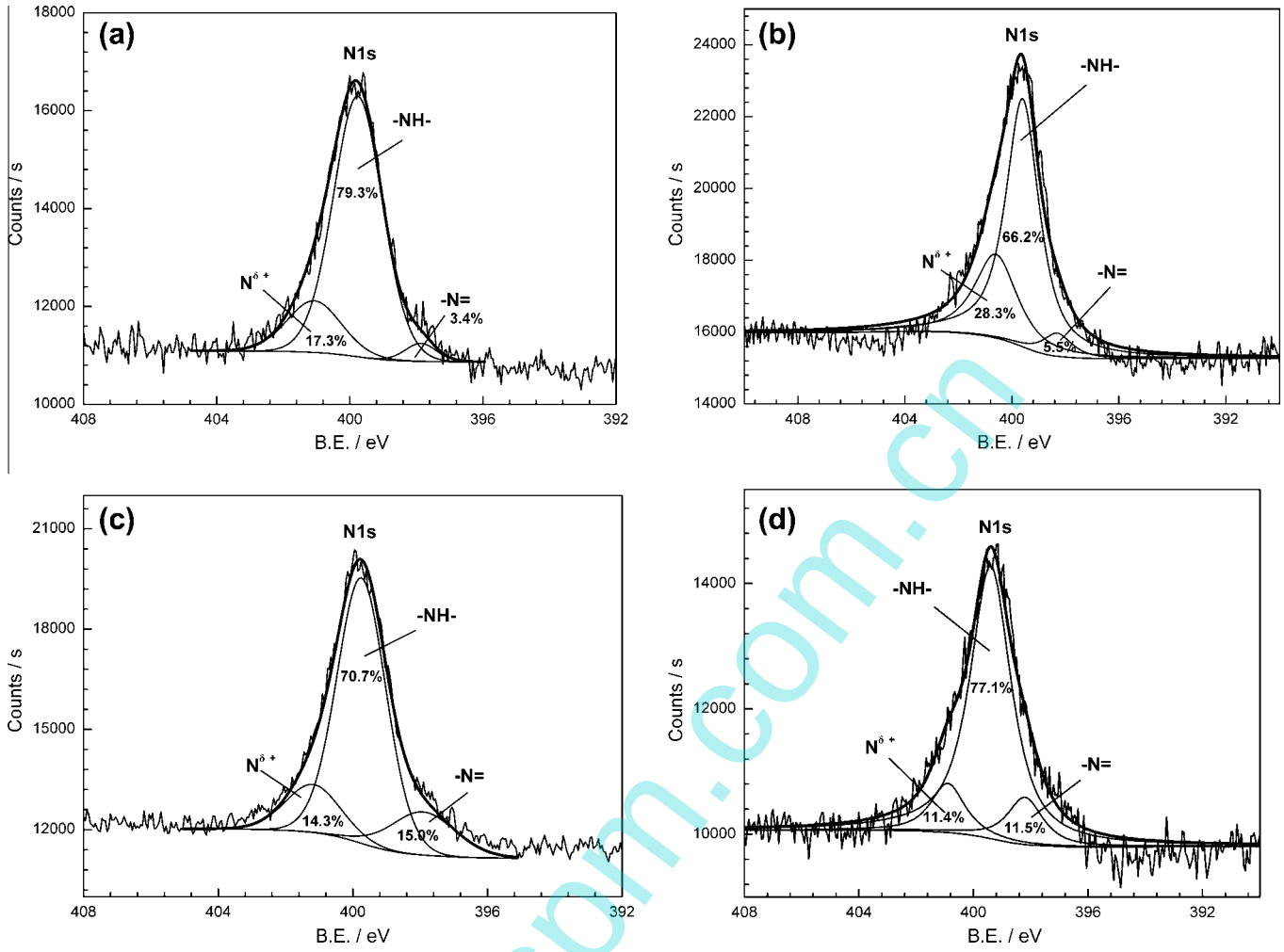

Fig. 7. XPS high resolution spectra of N 1s for (a) a PPy film immersed in deaerated 0.1 M NaCl for 75 h, (b) a PPy anode in the oxygen concentration difference cell in deaerated 0.1 M NaCl for 75 h, (c) a PPy film immersed in aerated 0.1 M NaCl for 75 h and (d) a PPy cathode in the oxygen concentration difference cell in aerated 0.1 M NaCl for 75 h.

larger than those in the acid solution (pH = 2) (=N—/N_{Total} ratio = 0.016 and 0.013, respectively). These results indicate that the PPy corrosion in the alkaline solution is much severer than that in the acid solution and the anodic polarisation does not accelerate the corrosion of the PPy anode obviously. However, the $N^{\delta+}/N_{Total}$ ratio of the PPy anode (0.168) increases obviously compared with that of the PPy film corroded under the free corrosion condition (0.122). This should result from the oxidation effect of the anodic current and lead to the increase in $\sigma_{pH\text{-}anode}$ (see Fig. 9).

In the acid deaerated 0.1 M NaCl (pH = 2), the two approximate =N—/N_{Total} ratios (see Table 3) demonstrate that the cathodic polarisation does not inhibit the corrosion of the PPy cathode. However, the $N^{\delta+}/N_{Total}$ ratio of the PPy cathode (0.186) decreases obviously compared with that of the PPy film just corroded under the free corrosion condition (0.317). Apparently, this should be due to the reduction effect of the cathodic current and lead to the decrease in $\sigma_{pH\text{-}cathode}$ (see Fig. 9).

3.4. Electrolyte (NaCl) concentration difference cell

As shown in Fig. 2, two identical PPy film electrodes were placed respectively in the cell A (with deaerated 1.0 M NaCl, pH = 7) and the cell B (with deaerated 0.1 M NaCl, pH = 7) to form the electrolyte (NaCl) concentration difference cell.

Fig. 11 shows the I_{couple}-t and E_{couple}-t curves of the electrolyte concentration difference cell. The E_{OCP}-t curve of each PPy electrode in the cell A and B is also presented respectively in Fig. 11(b). As shown in Fig. 11(a), I_{couple} decreases quickly after coupling and still maintains a smaller value of around 0.15 μA cm^{-2} when t_{couple} = 20 h, indicating that the electrolyte concentration difference cell can also be sustained on PPy films. The direction of I_{couple} and the E_{OCP} values in Fig. 11(b) indicate that the PPy film electrode in the cell A (1.0 M NaCl) acts as an anode and that in the cell B (0.1 M NaCl) acts as a cathode.

In Fig. 11(b), the E_{OCP} of the PPy film electrode in the cell A (1.0 M NaCl) is more negative than that in the cell B (0.1 M NaCl). Both of the E_{OCP} gradually decreases with time in the same way and may reach relatively stable after longer time conditioning, which may lead to the decrease in the E_{couple} with time.

Fig. 12 shows the electrical conductivity of the PPy anode and cathode in the electrolyte concentration difference cell for 40 h ($\sigma_{E\text{-}anode}$ and $\sigma_{E\text{-}cathode}$) and those just immersed in the corresponding solutions for the same time under free corrosion conditions (σ_{1M} and $\sigma_{0.1M}$). It can be seen that $\sigma_{E\text{-}anode}$ and σ_{1M} are smaller than $\sigma_{E\text{-}cathode}$ and $\sigma_{0.1M}$, suggesting that the corrosion of PPy in the deaerated 1.0 M NaCl may be severer than that in the deaerated 0.1 M NaCl. In addition, $\sigma_{E\text{-}anode}$ becomes larger than σ_{1M} because of the oxidation effect from anodic polarisation, while

www.spm.com.cn

Table 2
Ratios of $N^{\delta+}/N_{Total}$ and $=N-/N_{Total}$ obtained by quantitative analysis of XPS spectra for different PPy films in Fig. 7.

Samples	PPy film immersed in deaerated 0.1 M NaCl for 75 h	PPy anode in deaerated 0.1 M NaCl for 75 h	PPy film immersed in aerated 0.1 M NaCl for 75 h	PPy cathode in aerated 0.1 M NaCl for 75 h
$N^{\delta+}/N_{Total}$	0.173	0.283	0.143	0.114
$=N-/N_{Total}$	0.034	0.055	0.150	0.115

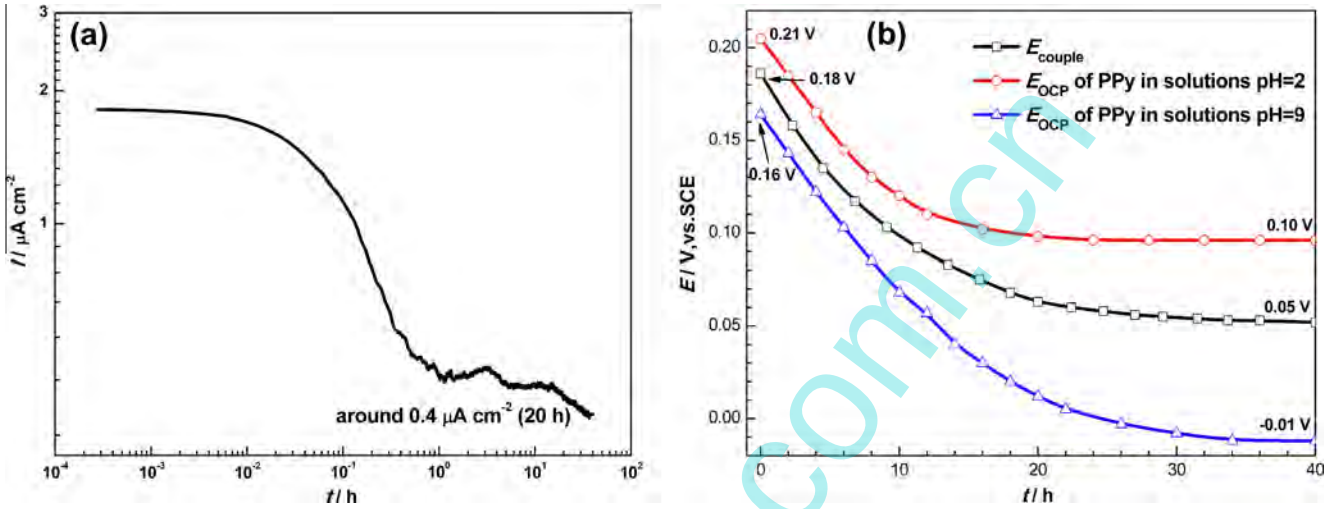

Fig. 8. (a) I_{couple}-t, (b) E_{couple}-t and E_{OCP}-t curves in the H^+ ion concentration difference cell (deaerated 0.1 M NaCl, pH = 2 and 9, at 25 °C).

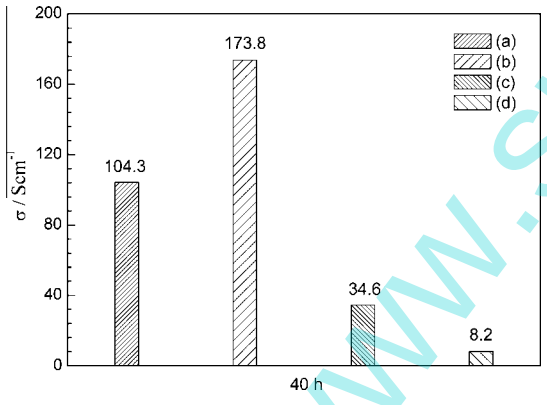

Fig. 9. Electrical conductivity (σ) for (a) a PPy cathode in the H^+ ion concentration difference cell in deaerated 0.1 M NaCl with pH = 2 ($\sigma_{pH\text{-}cathode}$) for 40 h, (b) a PPy film just immersed in deaerated 0.1 M NaCl with pH = 2 ($\sigma_{pH=2}$) for 40 h, (c) a PPy anode in the H^+ ion concentration difference cell in deaerated 0.1 M NaCl with pH = 9 ($\sigma_{pH\text{-}anode}$) for 40 h and (d) a PPy film just immersed in deaerated 0.1 M NaCl with pH = 9 ($\sigma_{pH=9}$) for 40 h.

$\sigma_{E\text{-}cathode}$ decreases slightly compared with $\sigma_{0.1M}$ owing to the reduction effect of cathodic polarisation.

Fig. 13 presents the high resolution XPS spectra of N 1s of the PPy anode and cathode in the electrolyte (NaCl) concentration difference cell for 40 h and those just immersed in the corresponding solutions for the same time under free corrosion conditions, where Table 4 gives the values of $N^{\delta+}/N_{Total}$ and $=N-/N_{Total}$ for the different PPy films obtained from Fig. 13. It is seen that in the deaerated 1.0 M NaCl the two $=N-/N_{Total}$ ratios are close to each other ($=N-/N_{Total}$ ratio = 0.032 and 0.033, respectively) and larger than those in the deaerated 0.1 M NaCl ($=N-/N_{Total}$ ratio = 0.021 and 0.019, respectively). These results indicate that the corrosion of PPy in the deaerated 1.0 M NaCl is severer than that in the deaerated 0.1 M NaCl and the anodic and cathodic polarisations have no obvious effects on the corrosion of PPy in the electrolyte (NaCl) concentration difference cell. However, the $N^{\delta+}/N_{Total}$ ratios for the PPy anode and PPy cathode are still affected obviously, resulting in the increase in $\sigma_{E\text{-}anode}$ and decrease in $\sigma_{E\text{-}cathode}$ (see Fig. 12). These results are consistent with those in the H^+ ion concentration difference cell.

4. Discussion

4.1. Factors affecting the E_{OCP} of a PPy film

The results in Figs. 4(b), 5(b), 8(b) and 11(b) indicate that the E_{OCP} of a PPy film electrode is related with its polarisation state and the concentrations of DO, H^+ ions and supporting electrolyte. It should be noted that it takes a relatively longer time for the E_{OCP} to reach stable in Figs. 5(b), 8(b) and 11(b). This may be mainly due to the higher electro-polymerisation potential (0.750 V_{SCE}), which results in a more positive initial E_{OCP} of the newly prepared PPy film (around 0.150–0.200 V_{SCE}). This may be seen as a depolarisation effect that can be similarly indicated by the results in Fig. 4(b). In addition, the response of the PPy film to the test media (such as DO, H^+ ions and supporting electrolyte) and the corrosion of PPy in the test media may also influence the stable E_{OCP}.

According to Refs. [40–44], the E_{OCP} of a PPy film in the electrolyte solutions can be described with a model equation, as shown in Eq. (1):

$$E_{OCP} = E^0 + \frac{RT}{F}\ln\frac{[Poly^{n+}]}{[Poly]} + \Delta\varphi_D \quad (1)$$

where E^0 is the standard potential of the redox system, $[Poly^{n+}]$ and [Poly] are concentrations of oxidized and reduced forms of PPy,

www.spm.com.cn

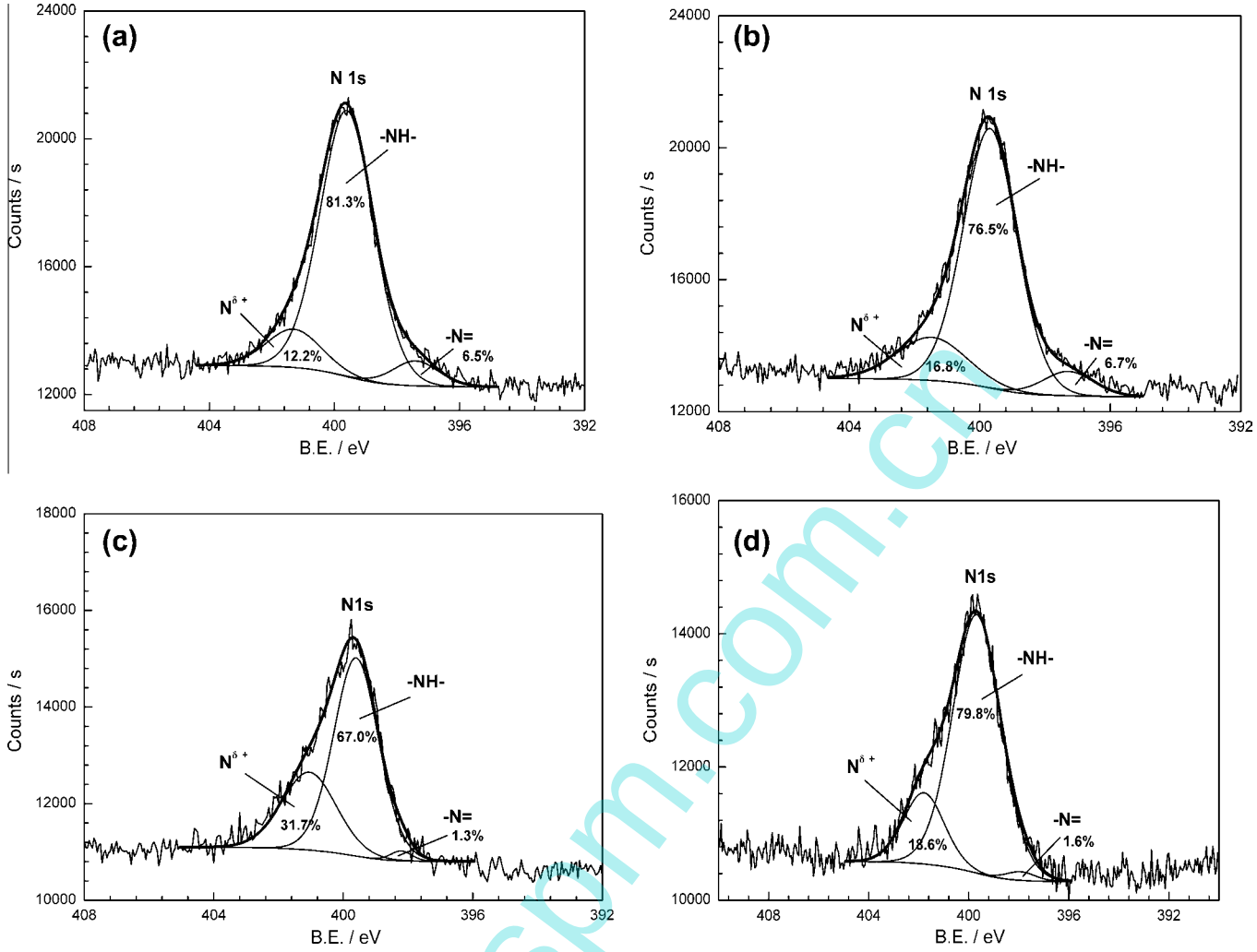

Fig. 10. XPS high resolution spectra of N 1s for (a) a PPy film just immersed in deaerated 0.1 M NaCl with pH = 9 for 40 h, (b) a PPy anode in the H^+ ion concentration difference cell in deaerated 0.1 M NaCl with pH = 9 for 40 h, (c) a PPy film just immersed in deaerated 0.1 M NaCl with pH = 2 for 40 h, and (d) a PPy cathode in the H^+ ion concentration difference cell in deaerated 0.1 M NaCl with pH = 2 for 40 h.

respectively, R is the standard gas constant, T is the temperature, F is the Faraday constant, and $\Delta\varphi_D$ is the Donnan potential on the polymer/solution interface. In aqueous electrolyte, the spontaneous charging/discharging processes on PPy affect its potential by changing $[Poly^{n+}]/[Poly]$ ratio according to Eq. (1). At a stable potential, the rates of charging and discharging processes are equal, and there is [41]:

$$k_{ox}[O_2][H^+]^p[Poly] = k_{red}[Poly^{n+}] \quad (2)$$

where k_{ox} and k_{red} are rate constants of polymer oxidation and reduction, respectively, $[O_2]$ and $[H^+]$ are concentrations of DO and H^+ ions, respectively, p is the reaction order. So, from Eq. (2) there is:

$$\frac{[Poly^{n+}]}{[Poly]} = \frac{k_{ox}}{k_{red}}[O_2][H^+]^p \quad (3)$$

In addition, $\Delta\varphi_D$ for PPy is described by the following Eq. (4) [45]:

$$\Delta\varphi_D = \frac{RT}{F}\ln\left\{\frac{X}{2c} + \left[1 + \left(\frac{X}{2c}\right)^2\right]^{\frac{1}{2}}\right\} \quad (4)$$

where X is the concentration of ion-exchange sites in the polymer and c is the concentration of supporting electrolytes.

Based on Eqs. (1), (3), and (4), there is:

$$E_{OCP} = E^0 + \frac{RT}{F}\ln\left\{\frac{k_{ox}}{k_{red}}[O_2][H^+]^p\right\} + \frac{RT}{F} \times \ln\left\{\frac{X}{2c} + \left[1 + \left(\frac{X}{2c}\right)^2\right]^{\frac{1}{2}}\right\} \quad (5)$$

It is seen that at a certain temperature the stable E_{OCP} of a PPy film is related to the concentrations of dissolved oxygen ($[O_2]$), H^+ ions ($[H^+]$) and supporting electrolyte (c).

According to Eq. (5), a PPy film in acid solutions (with higher $[H^+]$) has more positive E_{OCP}. This may be owing to the higher doping level of H^+ ions for the PPy film in the acid solutions because one kind of doping site on PPy chains is related to a protonated Py unit [46]. In this case, the PPy film maintains a higher oxidation state. The influence of the concentration of supporting electrolyte (c) is apparently attributed to the change of $\Delta\varphi_D$, while the effect of DO should be attributed to the redox couple of O_2/OH^- on the PPy film [32,33,41]. From the qualitative point of view, Eq. (5) can explain the effects of $[O_2]$, $[H^+]$ and c on the stable E_{OCP} of the PPy film, which is verified with the results in Figs. 5(b), 8(b) and 11(b).

However, because of the corrosion of PPy, the redox state of PPy is changing with time and difficult to reach stable. In this case,

www.spm.com.cn

Table 3
Ratios of $N^{\delta+}/N_{Total}$ and $=N-/N_{Total}$ obtained by quantitative analysis of XPS spectra for different PPy films in Fig. 10.

Samples	PPy film immersed in deaerated 0.1 M NaCl with pH = 9 for 40 h	PPy anode in deaerated 0.1 M NaCl with pH = 9 for 40 h	PPy film immersed in deaerated 0.1 M NaCl with pH = 2 for 40 h	PPy cathode in deaerated 0.1 M NaCl with pH = 2 for 40 h
$N^{\delta+}/N_{Total}$	0.122	0.168	0.317	0.186
$=N-/N_{Total}$	0.065	0.067	0.013	0.016

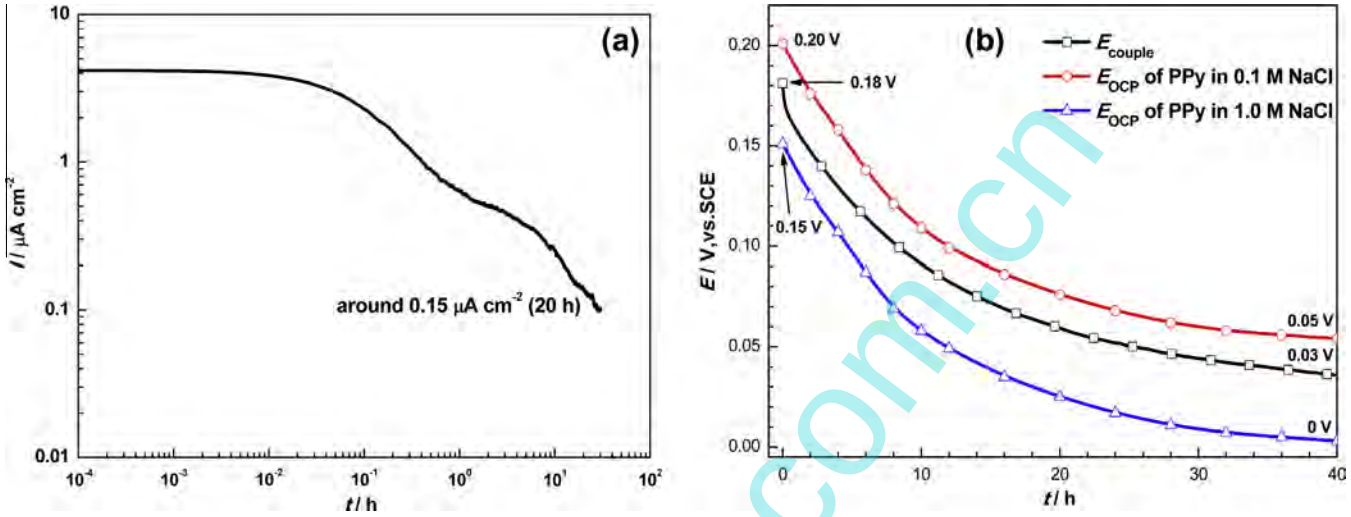

Fig. 11. (a) I_{couple}-t, (b) E_{couple}-t and E_{OCP}-t curves in the electrolyte concentration difference cell (deaerated 1.0 M and 0.1 M NaCl, pH = 7, at 25 °C).

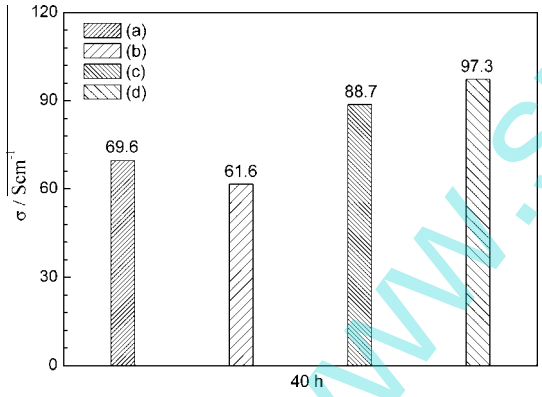

Fig. 12. Electrical conductivity (σ) for (a) a PPy anode in the electrolyte concentration difference cell in deaerated 1.0 M NaCl for 40 h ($\sigma_{E\text{-anode}}$), (b) a PPy film just immersed in deaerated 1.0 M NaCl for 40 h (σ_{1M}), (c) a PPy cathode in the electrolyte concentration difference cell in deaerated 0.1 M NaCl for 40 h ($\sigma_{E\text{-cathode}}$) and (d) a PPy film just immersed in deaerated 0.1 M NaCl for 40 h ($\sigma_{0.1M}$).

large deviation will occur in Eq. (5). In addition, it is possible to form corrosion cells on PPy films, just liking those on metals and, therefore, the stable E_{OCP} is also determined by the anodic and cathodic processes on the PPy film, which is similar to the E_{couple} in Figs. 4(b), 5(b), 8(b) and 11(b).

4.2. Formation of galvanic cells on PPy films

For a freshly electro-polymerised PPy film, its redox state or the doping ratio cannot be completely uniform, i.e. there is different ratios of $[Poly^{n+}]/[Poly]$ at different locations of the PPy film, which results in different potentials according to Eq. (1). So the PPy redox state difference cell will occur on the PPy film. However, as shown in Fig. 4(a), this galvanic cell cannot be sustained for a long time. Apart from the polarisation effect, the spontaneous oxidation of reduced PPy and discharge of oxidized PPy [41] will also gradually eliminate the redox state difference on the PPy film. So, this kind of the corrosion cell just occurs in the initial corrosion period (such as 5 h) for a newly made PPy film.

In addition, the porous structure of a PPy film is also not uniform and, therefore, its density (porosity, thickness, etc.) in different locations will not be identical. In this case, a nonuniform distribution of molecules (e.g. O_2) and other ions (H^+, Na^+, Cl^-, OH^-, etc.) can be assumed in the PPy membrane [41]. Fig. 14 shows the schematic of the nonuniform distribution of molecules and ions in a PPy film. Apparently, the concentrations of various molecules and ions near the PPy outer surface are the highest, while those in the PPy film, especially in the more compact PPy area, are lower because those molecules and ions diffuse to the inner film with difficulty. So the oxygen concentration difference cell, the H^+ ion concentration difference cell and the electrolyte (NaCl) concentration difference cell can occur on PPy films.

For the oxygen concentration difference cell formed on PPy films, the anodic and cathodic reactions can be expressed as:

$$\text{Anodic reaction}: \ PPy^{n+}/npTS^- + xCl^- \rightleftarrows PPy^{(n+x)+}/npTS^-xCl^- + xe^- \quad (6)$$

$$\text{Cathodic reaction}: \ O_2 + 2H_2O + 4e^- \rightarrow 4OH^- \quad (7)$$

$$PPy^{n+}/npTS^- + ye^- + yNa^+ \rightleftarrows PPy^{(n-y)+}/npTS^-yNa^+ (y < x) \quad (8)$$

where the arrow "$\rightleftarrows$" means that PPy has the spontaneous charging/discharging tendency to recover partly after anodic or cathodic polarisation.

The main cathodic process is the reduction of dissolved oxygen on the PPy film. However, because the electron flows through PPy

www.spm.com.cn

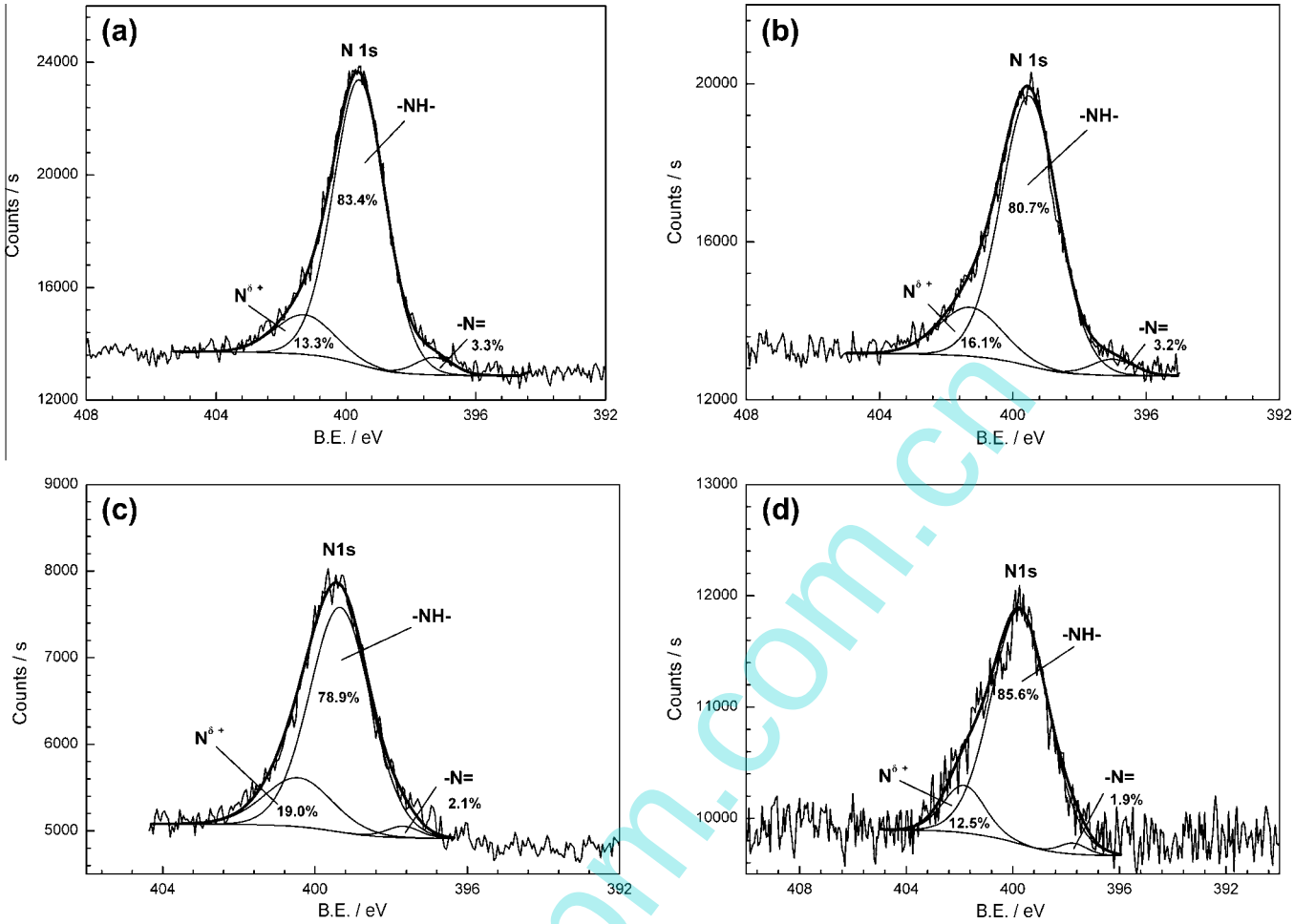

Fig. 13. XPS high resolution spectra of N 1s for (a) a PPy film just immersed in deaerated 1.0 M NaCl for 40 h, (b) a PPy anode in the electrolyte concentration difference cell in deaerated 1.0 M NaCl for 40 h, (c) a PPy film just immersed in deaerated 0.1 M NaCl for 40 h and (d) a PPy cathode in the electrolyte concentration difference cell in deaerated 0.1 M NaCl for 40 h.

Table 4
Ratios of $N^{\delta+}/N_{Total}$ and $=N-/N_{Total}$ obtained by quantitative analysis of XPS spectra for different PPy films in Fig. 13.

Samples	PPy film immersed in deaerated 1.0 M NaCl for 40 h	PPy anode in deaerated 1.0 M NaCl for 40 h	PPy film immersed in deaerated 0.1 M NaCl for 40 h	PPy cathode in deaerated 0.1 M NaCl for 40 h
$N^{\delta+}/N_{Total}$	0.133	0.161	0.190	0.125
$=N-/N_{Total}$	0.033	0.032	0.021	0.019

chains, the reduction of PPy cathode also occurs to some extent, including the decrease of the positive charge in the polymeric lattice and incorporation of cations (Na^+). The reduction effect will weaken the attack of OH^- ions generated from Eq. (7), owing to the less positive charge sites, so as to depress the corrosion of PPy cathode. This effect will also decrease the conductivity of PPy cathode. However, the OH^- ions may diffuse to the neighbouring area and attack the PPy chains to break their conjugated structures [33], which will create severe corrosion.

The anodic process is the oxidation of PPy including the creation of more positive charge in the polymer and incorporation of anions (Cl^-), as shown in Eq. (6). However, under the continuous anodic polarization, chlorine substitution occurs at the β-position of the pyrrole ring owing to the nucleophilic property of Cl^- ions. Then the hydrolysis occurs to make C—Cl substituted by hydroxides C—OH, and finally the hydroxylation of PPy forms carbonyl groups to break the conjugated structure of PPy chains [33,47,48]. Therefore, the corrosion of PPy anode is accelerated. Fig. 15 presents the high resolution XPS spectra of Cl 2p and O 1s for a PPy anode of the oxygen concentration difference cell in deaerated 0.1 M NaCl for 75 h, which further prove the existence of C—Cl and C—OH bonds in the PPy chains.

For the H^+ ion concentration difference cell formed on PPy films, the anodic and cathodic reactions can be expressed as:

$$\text{Anodic reaction}: \ PPy^{(n+g)+}/npTS^- gCl^- + xCl^- \rightleftarrows PPy^{(n+g+x)+}/npTS^-(g+x)Cl^- + xe^- \quad (9)$$

$$\text{Cathodic reaction}: \ PPy^{(n+j)+}/npTS^- jCl^- + xe^- \rightleftarrows PPy^{(n+j-x)+}/npTS^-(j-x)Cl^- + xCl^- \quad (10)$$

where g and j ($0 \leqslant g < j$) represent the protonic acid doping level of H^+ ions.

www.spm.com.cn

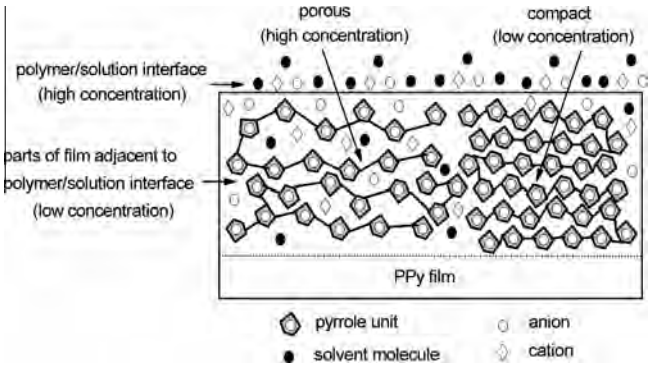

Fig. 14. Schematic of the nonuniform distribution of molecules and ions in a PPy film.

When the H^+ ion concentration difference cell is formed on PPy films, the PPy anode and cathode polarises with each other and their potential difference decreases to lower the galvanic current. If the potential difference disappears, the galvanic current should decrease to zero, just like that in the PPy redox state difference cell. However, it maintains a small stable value, as shown in Fig. 8(a). This should be related to spontaneous charging and discharging processes on PPy films. For example, the PPy cathode in a reduced state has the spontaneous tendency of charging-oxidation-redoping, which will gradually increase $(n+j-x)$ to $(n+j)$ again (see Eq. (10)) and make the PPy cathode depolarised to some extent, while the PPy anode in an oxidized state has the spontaneous tendency of discharging-reduction-dedoping, which will gradually decrease $(n+g+x)$ to $(n+g)$ again (see Eq. (9)) and impede the anodic polarisation of PPy anode. In this case, the potential difference between the PPy cathode and anode cannot be eliminated unless the pH difference disappears, so a steady-state galvanic current remains from the dedoping-redoping dynamic equilibrium process between the PPy anode and cathode. However, the gain and loss of electron just occur in the PPy itself and the galvanic current density is too small, so the galvanic current has no obvious effects on the corrosion of PPy (see Table 3).

For the electrolyte (NaCl) concentration difference cell formed on PPy films, the anodic and cathodic reactions can be expressed as:

$$\text{Anodic reaction}: \ PPy^{n+}/n pTS^- + xCl^- \rightleftarrows PPy^{(n+x)+}/n pTS^- xCl^- + xe^- \quad (11)$$

$$\text{Cathodic reaction}: \ PPy^{n+}/n pTS^- + xe^- + xNa^+ \rightleftarrows PPy^{(n-x)+}/n pTS^- xNa^+ \quad (12)$$

where the PPy anode has a lower $\Delta\varphi_{D1}$, while the PPy cathode has a higher $\Delta\varphi_{D2}$.

Being similar to the H^+ ion concentration difference cell, in the electrolyte (NaCl) concentration difference cell, the PPy anode in an oxidized state has the spontaneous tendency of discharging-reduction-dedoping, which will decrease $(n+x)$ (see Eq. (11)); while the PPy cathode in a reduced state has the spontaneous tendency of charging-oxidation-redoping, which will increase $(n-x)$ (see Eq. (12)). In this case, both of the PPy anode and cathode are depolarised to some extent so that the potential difference between them cannot be eliminated unless the electrolyte (NaCl) concentration difference disappears. This dedoping-redoping dynamic equilibrium process between the PPy anode and cathode causes a steady-state galvanic current, which also has no obvious effects on the corrosion of PPy (see Table 4).

4.3. The potential distribution on the PPy film surface

Fig. 16 shows the potential distribution on the same area (1 mm × 1 mm) of a PPy film surface immersed in aerated 0.1 M NaCl for different time (0–44 h), which was measured with a XMU-BY-1 scanning electrochemical workstation system. It is seen that the potentials on different locations of the measuring area are not same at first and gradually become uniform after 6 h of immersion, as shown in Fig. 16(a–d). However, after 20 h of immersion the potential distribution becomes nonuniform again and gradually develops with the increase in the immersion time, as shown in Figs. 16(e–h). The maximum potential difference in the test surface reaches 20 mV. This result proves that the potential difference occurs on the PPy film and can be maintained for a long time. In this case, corrosion cells can be formed on the PPy film.

In the initial immersion period (0–6 h), the change of the potential distribution may be due to the redox state difference on the PPy film. In this period, the PPy redox state difference cell occurs firstly on the PPy film and then gradually disappears, displaying a uniform potential distribution, as shown in Fig. 16(d). With an increase in the immersion time to more than 6 h, the molecules and ions (H_2O, O_2, Na^+, Cl^-, H^+, etc.) penetrate into the PPy film and the oxygen concentration difference cell, the H^+ ion concentration difference cell, and the electrolyte (NaCl) concentration difference cell gradually form on the PPy film. As a result of the comprehensive effects of these corrosion cells, the potential distri-

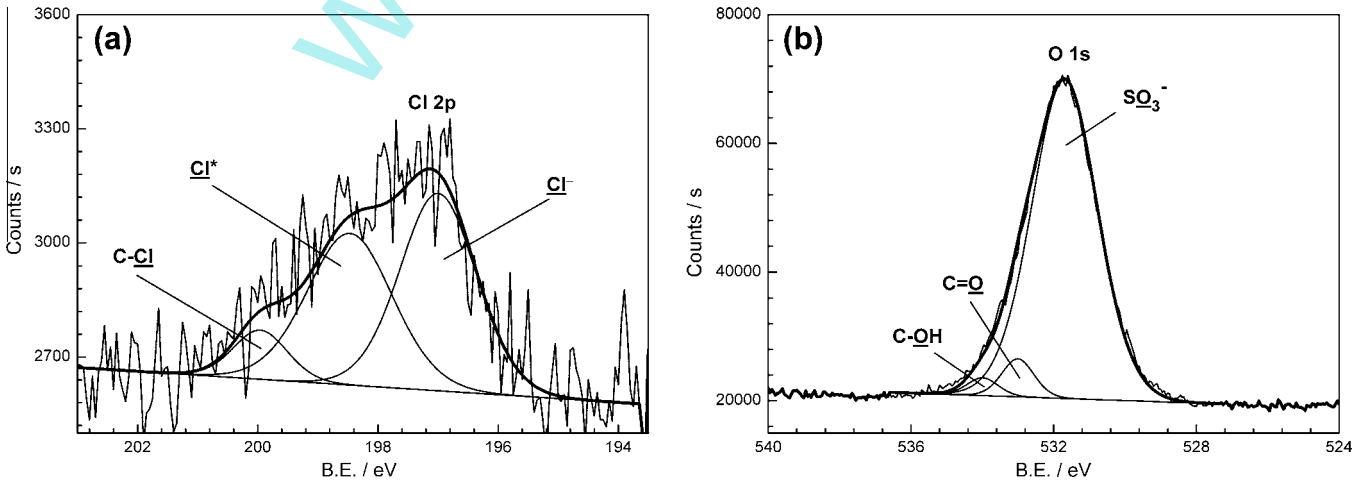

Fig. 15. XPS high resolution spectra of (a) Cl 2p and (b) O 1s for a PPy anode of the oxygen concentration difference cell in deaerated 0.1 M NaCl for 75 h.

www.spm.com.cn

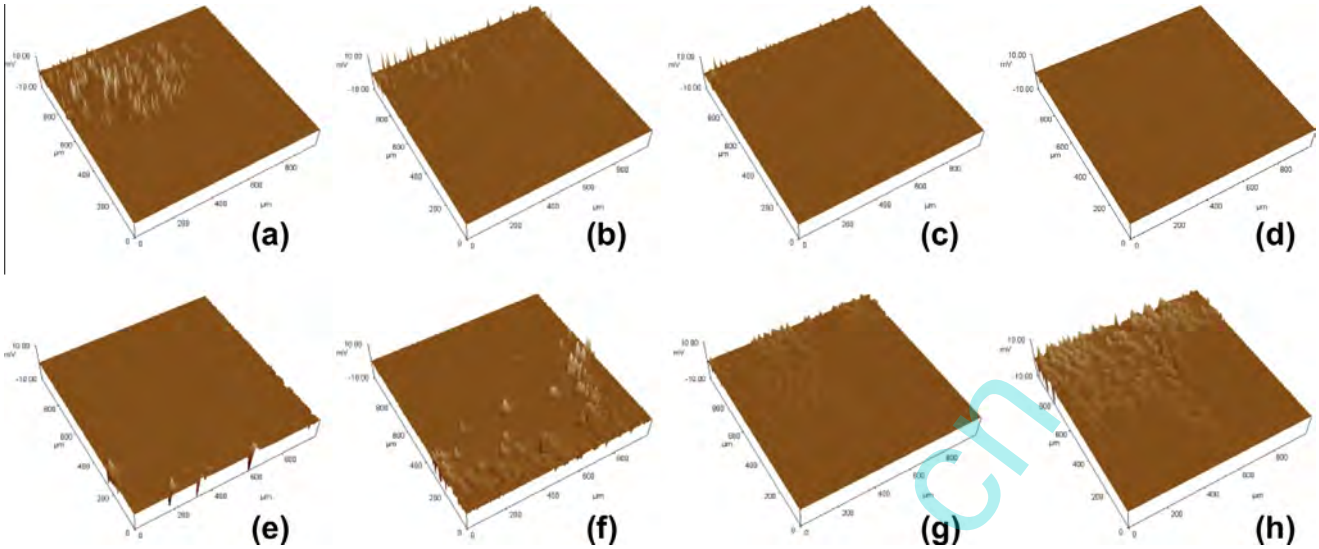

Fig. 16. 3D images (1 mm × 1 mm) of the potential distribution on the same area of a PPy film surface immersed in aerated 0.1 M NaCl for (a) 0 h; (b) 3 h; (c) 5 h; (d) 6 h; (e) 20 h; (f) 26 h; (g) 31 h and (h) 44 h.

bution on the PPy film gradually becomes nonuniform again and develops with the immersion time. However, according to our experimental results and discussion, it should be noted that the H^+ ion concentration difference cell and the electrolyte (NaCl) concentration difference cell have no obvious influences on the corrosion of PPy, while the oxygen concentration difference cell accelerates the corrosion of PPy severely.

5. Conclusions

In this paper, some galvanic couples were formed with PPy electrodes to simulate possibly formed corrosion cells on the PPy films. Their effects on the conductivity and corrosion of PPy were investigated using electrochemical methods and XPS analysis. The following conclusions are drawn from the results of experiments:

(1) The PPy redox state difference cell, the oxygen concentration difference cell, the H^+ ion concentration difference cell and the electrolyte (NaCl) concentration difference cell can occur on the PPy films in electrolyte solutions.
(2) Under the studied conditions, the PPy redox state difference cell just occurs in the initial corrosion period and cannot be sustained for a long time (such as more than 5 h). The other three kinds of corrosion cells can be sustained for a longer time (such as more than 40 h).
(3) The formation of the oxygen concentration difference cell on PPy films will obviously influence the conductivity and corrosion of PPy. In this corrosion cell, the cathodic processes include the reduction of DO and PPy itself, which make the PPy cathode in the reduction state and decrease its conductivity. The OH^- ions generated from the reduction of DO attack PPy and result in the severe corrosion of PPy. At the same time, the corrosion of the PPy anode is accelerated owing to the breakdown of the PPy conjugated structure by the anodic polarisation, which also decreases the conductivity of the PPy anode. In aerated electrolyte solutions, the oxygen concentration difference cell formed on the PPy films plays an important role in the corrosion of PPy.
(4) The formation of the H^+ ion concentration difference cell and the electrolyte (NaCl) concentration difference cell on PPy films has no obvious effect on the corrosion of PPy under the test condition, but still has some slight influence on its conductivity. However, the conductivity of a PPy film does not directly reflect its corrosion extent.

Acknowledgements

We appreciate the analysis support of Center of Forecasting and Analysis, Huazhong University of Science and Technology.

References

[1] L. Valero, J. Arias-Pardilla, J. Cauich-Rodríguez, M.A. Smit, T.F. Otero, Characterization of the movement of polypyrrole dodecylbenzenesulfonate perchlorate/tape artificial muscles. Faradaic control of reactive artificial molecular motors and muscles, Electrochim. Acta 56 (2011) 3721–3726.
[2] D.P. Dubal, S.V. Patil, A.D. Jagadale, C.D. Lokhande, Two step novel chemical synthesis of polypyrrole nanoplates for supercapacitor application, J. Alloys. Compd. 509 (2011) 8183–8188.
[3] S.S. Jeon, H.H. An, C.S. Yoon, S.S. Im, Synthesis of ultra thin polypyrrole nanosheets for chemicalsensor applications, Polymer 52 (2011) 652–657.
[4] H.Y. Qin, Z.X. Liu, L.Q. Ye, J.K. Zhu, Z.P. Li, The use of polypyrrole modified carbon-supported cobalt hydroxide as cathode and anode catalysts for the direct borohydride fuel cell, J. Power Sources 192 (2009) 385–390.
[5] M.B. González, S.B. Saidman, Electrodeposition of polypyrrole on 316L stainless steel forcorrosion prevention, Corros. Sci. 53 (2011) 276–282.
[6] D.T. Ge, X.D. Tian, R.C. Qi, S.Q. Huang, J. Mu, S.M. Hong, S.F. Ye, X.M. Zhang, D.H. Li, W. Shi, A polypyrrole-based microchip for controlled drug release, Electrochim. Acta 55 (2009) 271–275.
[7] H. Hammache, L. Makhloufi, B. Saidani, Corrosion protection of iron by polypyrrole modified by copper using the cementation process, Corros. Sci. 45 (2003) 2031–2042.
[8] R.K. Sharma, A.C. Rastogi, S.B. Desu, Pulse polymerized polypyrrole electrodes for high energy density electrochemical supercapacitor, Electrochem. Commun. 10 (2008) 268–272.
[9] A.A. Pud, Stability and degradation of conducting polymers in electrochemical systems, Synth. Met. 66 (1994) 1–18.
[10] I. Fernandez, M. Trueba, C.A. Nunez, J. Rieumont, Some features of the overoxidation of polypyrrole synthesized on austenitic stainless steel electrodes in aqueous nitrate solutions, Surf. Coat. Technol. 191 (2005) 134–139.
[11] http://www.efcweb.org/Working+Parties/WP+19.html (19.09.11).
[12] P.S. Abthagir, R. Saraswathi, Thermal stability of polypyrrole prepared from a ternary eutectic melt, Mater. Chem. Phys. 92 (2005) 21–26.
[13] A. Yfantis, G. Appel, D. Schmeiber, D. Yfantis, Polypyrrole doped with fluro-metal composites: thermal stability and structural properties, Synth. Met. 106 (1997) 187–195.
[14] F. Cataldo, M. Omastova, On the ozone degradation of polypyrrole, Polym. Degrad. Stab. 82 (2003) 487–495.
[15] A. Alumaa, A. Hallik, V. Sammelselg, J. Tamm, On the improvement of stability of polypyrrole films in aqueous solutions, Synth. Met. 157 (2007) 485–491.

[16] Ying Tian, Fenglin Yang, Weishen Yang, Redox behavior and stability of polypyrrole film in sulfuric acid, Synth. Met. 156 (2006) 1052–1056.
[17] Mohamed M. Chehimi, Essadik Abdeljalil, A study of the degradation and stability of polypyrrole by inverse gas chromatography, X-ray photoelectron spectroscopy, and conductivity measurements, Synth. Met. 145 (2004) 15–22.
[18] Jorge G. Ibanez, Alejandro Alatorre-Ordaz, Silvia Gutierrez-Granados, Nikola Batina, Nanoscale degradation of polypyrrole films under oxidative stress: an atomic force microscopy study and review, Polym. Degrad. Stab. 93 (2008) 827–837.
[19] Soumyadeb Ghosh, Graham A. Bowmaker, Ralph P. Cooney, John M. Seakins, Infrared and Raman spectroscopic studies of the electrochemical oxidative degradation of polypyrrole, Synth. Met. 95 (1998) 63–67.
[20] Y.C. Liu, B.J. Hwang, Mechanism of conductivity decay of polypyrrole exposed to water and enhancement of conductivity stability of copper(I)-modified polypyrrole, J. Electroanal. Chem. 501 (2001) 100–106.
[21] Y. Li, R. Qian, Electrochemical overoxidation of conducting polypyrrole nitrate film in aqueous solutions, Eletrochim. Acta 45 (2000) 1727–1731.
[22] J. Mostany, B.R. Scharifker, Direct microcalorimetric measurement of doping and overoxidation process in polypyrrole, Electrochim. Acta 42 (1997) 291–301.
[23] I. Rodriguez, B.R. Scharifker, J. Mostany, In situ FTIR study of redox and overoxidation processes in polypyrrole films, J. Electroanal. Chem. 491 (2000) 117–125.
[24] H. Xie, M. Yan, Z. Jiang, Transition of polypyrrole from electroactive to electroinactive state investigated by use of in situ FTIR spectroscopy, Electrochim. Acta 42 (1997) 2361–2367.
[25] K.G. Neoh, T.T. Young, E.T. Kang, et al., Structural and mechanical degradation of polypyrrole films due to aqueous media and heat treatment and the subsequent redoping characteristics, J. Appl. Polym. Sci. 64 (1997) 519–526.
[26] G.G. Wallace, G.M. Spinks, L.A.P. Kane-Maguire, P.R. Teasdale, Conductive Electroactive Polymers: Intelligent Polymer Systems, Taylor & Francis, Boca Raton, 2009.
[27] A. Malinauskas, Electrocatalysis at conducting polymers, Synth. Met. 107 (1999) 75–83.
[28] A. Haimeri, A. Merz, Catalysis of quinone-hydroquinone redox reactions at polypyrrole benzenesulofnate-coated platinum-electrodes, J. Electroanal. Chem. 220 (1987) 55–65.
[29] W. Schuhmann, R. Lammert, M. Hammerle, H.-L. Schmidt, Elecrtocatalytic properties of polypyrrole in amperometric electrodes, Biosens. Bioelecrton. 6 (1991) 689–697.
[30] M. Kwaashima, Y. Sato, M. Sato, M. Sakaguchi, Role of catalysts on electrode activity in oxygen diuffsion hybrid polymer electrode, Polym. J. 23 (1991) 37–45.
[31] B. Zinger, Electrochemistry of quinoid dopants in conducting polymers, Synth. Met. 30 (1989) 209–225.
[32] K. Qi, Y.B. Qiu, Z.Y. Chen, X.P. Guo, Corrosion of conductive polypyrrole: effects of environmental factors, electrochemical stimulation, and doping anions, Corros. Sci. 60 (2012) 50–58.
[33] K. Qi, Y.B. Qiu, Z.Y. Chen, X.P. Guo, Corrosion of conductive polypyrrole: effects of continuous cathodic and anodic polarisation, Corros. Sci. 69 (2013) 376–388.
[34] B. Lin, R.G. Hu, C.Q. Ye, Y. Li, C.J. Lin, A study on the initiation of pitting corrosion in carbon steel in chloride-containing media using scanning electrochemical probes, Eletrochim. Acta 55 (2010) 6542–6545.
[35] J. Molina, J. Fernández, A.I. del Río, R. Lapuente, J. Bonastre, F. Cases, Stability of conducting polyester/polypyrrole fabrics in different pH solutions: chemical and electrochemical characterization, Polym. Degrad. Stab. 95 (2010) 2574–2583.
[36] Ramakrishnan Rajagopalan, Jude O. Iroh, Characterization of polyaniline–polypyrrole composite coatings on low carbon steel: a XPS and infrared spectroscopy study, Appl. Surf. Sci. 218 (2003) 58–69.
[37] Stephanie Carquigny, Olivier Segut, Boris Lakard, F. Lallemand, Patrick Fievet, Effect of electrolyte solvent on the morphology of polypyrrole films: application to the use of polypyrrole in pH sensors, Synth. Met. 158 (2008) 453–461.
[38] Walaiporn Prissanaroon-Ouajai, Paul J. Pigram, Robert Jones, Anuvat Sirivat, A novel pH sensor based on hydroquinone monosulfonate-doped conducting polypyrrole, Sens. Actuators. B 135 (2008) 366–374.
[39] Q.B. Pei, R.Y. Qian, Protonation and deprotonation of polypyrrole chain in aqueous solutions, Synth. Met. 45 (1991) 35–48.
[40] K. Doblhofer, The non-metallic character of solvated conducting polymers, J. Electroanal. Chem. 331 (1992) 1015–1027.
[41] J. Dumanska, K. Maksymiuk, Studies on spontaneous charging/discharging processes of polypyrrole in aqueous electrolyte solutions, Electroanalysis 13 (2001) 567–573.
[42] A. Lewenstam, J. Bobacka, A. Ivaska, Mechanism of ionic and redox sensitivity of *p*-type conducting polymers Part 1. Theory, J. Electroanal. Chem. 368 (1994) 23–31.
[43] J. Bobacka, Z.Q. Gao, A. Ivaska, A. Lewenstam, Mechanism of ionic and redox sensitivity of *p*-type conducting polymers Part 2. Experimental study of polypyrrole, J. Electroanal. Chem. 368 (1994) 33–41.
[44] A. Alumaa, A. Hallik, V. Sammelselg, J. Tamm, On the improvement of stability of polypyrrole films in aqueous solutions, Synth. Met. 157 (2007) 485–491.
[45] K.J. Vetter, Electrochemical Kinetics, Academic Press, New York, 1967.
[46] Y.F. Li, R.Y. Qian, On the nature of redox processes in the cyclic voltammetry of polypyrrole nitrate in aqueous solutions, J. Electroanal. Chem. 362 (1993) 267–272.
[47] Z. Qi, N.G. Rees, P.G. Pickup, Electrochemically induced substitution of polythiophenes and polypyrrole, Chem. Mater. 8 (1996) 701–707.
[48] S. Ghosh, G.A. Bowmaker, R.P. Cooney, J.M. Seakins, Infrared and Raman spectroscopic studies of the electrochemical oxidative degradation of polypyrrole, Synth. Met. 95 (1998) 63–67.

www.spm.com.cn